

基于不同 S-N 曲线的横向十字焊接接头 疲劳寿命预测

范文学^{1,2}, 陈芙蓉¹, 解瑞军¹, 高 健¹

(1. 内蒙古工业大学 材料科学与工程学院, 呼和浩特 010051; 2. 内蒙古工业大学 矿业学院, 呼和浩特 010051)

摘 要: 通过疲劳分析软件 MSC. Fatigue 自动生成了 3 种不同 S-N 曲线, 即试验 S-N 曲线、经验 S-N 曲线和标准 S-N 曲线, 考虑了残余应力、平均应力、接头外形对焊接疲劳的影响, 并按相关规则修正后对碳钢 Q235B 十字焊接接头进行了疲劳寿命预测, 并进行了比较分析。结果表明, 基于 MSC. Fatigue 的 S-N 曲线法模拟的焊接接头疲劳损伤部位及损伤程度与试验结果一致; 试验 S-N 曲线预测值与标准 S-N 曲线预测值偏差在 7.9%~28%, 与经验 S-N 曲线预测值偏差 3.3%~19%, 经验 S-N 曲线预测结果偏高, 而标准 S-N 曲线预测结果相对比较保守。

关键词: 十字焊接接头; 疲劳寿命; 有限元分析; S-N 曲线

中图分类号: TG405 **文献标识码:** A **文章编号:** 0253-360X(2013)11-0069-04



范文学

0 序 言

疲劳是焊接结构破坏的主要形式之一, 传统的疲劳试验分析法由于其耗资大、时间长已无法完全满足疲劳的研究。目前借助有限元法评定焊接结构的疲劳强度受到很多学者的青睐。贾法勇等人^[1]通过有限元法获得了双相不锈钢焊接结构的热点 S-N 曲线, 并确定了热点疲劳强度。武奇等人^[2]利用有限元法推断了结构应力计算公式并实现接头的疲劳评定。于海丰等人^[3]借助有限元法对 Q235 材质焊接工字钢进行数值模拟, 结果偏小于实测数据, 但基本分散在 4 倍以内。王文先等人^[4]通过有限元法对比分析, 说明热点 S-N 曲线具有较小的分散性。

多数焊接结构疲劳分析均通过有限元法进行应力分布的求解, 然后利用试验获取疲劳数据并进行回归计算, 确定材料或结构的应力 S-N 曲线, 并计算其疲劳强度。但很少有文献提到通过疲劳分析软件来生成相应 S-N 曲线, 实现疲劳的分析。为了减少投资、加快研究进度, 以数值模拟代替实际疲劳试验获取相关数据显得尤为必要。为此文中通过 MSC. Fatigue 生成不同的 S-N 曲线, 对 Q235B 十字焊接接头进行疲劳寿命预测。

1 疲劳分析的准备工作的

1.1 材料及接头形式

结构钢 Q235B 是工程中常用的焊接结构用钢, 破坏形式主要是疲劳断裂, 所以文中选用板材尺寸为 200 mm × 80 mm × 8 mm 和 80 mm × 25 mm × 8 mm 的 Q235B 低碳钢板, 焊条采用 E5015, 直径均为 4 mm, 其力学性能见表 1。

表 1 试验材料的力学性能

Table 1 Mechanical property of test materials

| 材料 | 屈服强度 R_{eL}/MPa | 抗拉强度 R_m/MPa | 弹性模量 E/MPa | 泊松比 μ |
|-------|-----------------------------|--------------------------|------------------------|--------------|
| Q235B | 265 | 415 | 2.06×10^5 | 0.26 |
| E5015 | 457 | 552 | 2.10×10^5 | 0.30 |

1.2 焊接过程及试样制备

焊缝采用单层不开破口的平角焊缝。焊接过程采用侧面定位, 主板两侧交替焊接, 由试板边缘起弧、熄弧。焊接工艺参数如表 2 所示。图 1 为横向十字焊接接头几何特征。

1.3 疲劳试验及数据处理

表 3 为疲劳试验数据。疲劳试验是在 GPS300 型高频疲劳试验机上进行。应力循环比为 $R=0.1$, 振动频率控制在 $f=130 \sim 140 \text{ Hz}$ 的范围内。

接头在 2×10^6 周次循环时的疲劳值。

表 4 疲劳 S-N 曲线参数

Table 4 Parameters of fatigue S-N Curve

| 曲线 | 斜率 b | 应力范围截距 C_1 /MPa |
|--------|----------|-------------------|
| 试验 S-N | -0.098 9 | 685.18 |
| 标准 S-N | -0.333 3 | 10 100.00 |
| 经验 S-N | -0.155 1 | 1 939.00 |

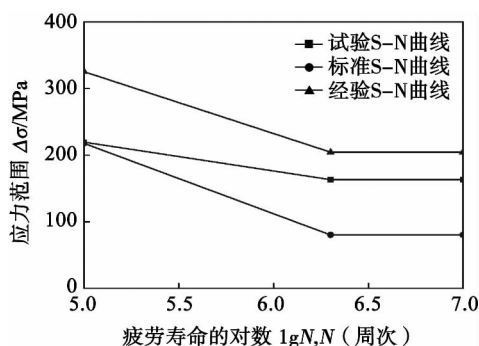


图 3 3 种 S-N 曲线

Fig. 3 Three kinds of S-N curves

2.5 不同 S-N 曲线的对比分析

图 3 中的 3 条 S-N 曲线在 2×10^6 周次时, 试验 S-N 曲线的疲劳强度为 163.17 MPa, 经验 S-N 曲线的疲劳强度为 227.498 MPa, 标准 S-N 曲线的疲劳强度为 80 MPa。

国际焊接学会推荐的标准疲劳强度要表达同种材料、相似的多个焊接接头的疲劳强度, 所以比较保守。该值是在 $R = -1$ 的情况下得到, 要对其进行 Goodman^[7] 修正才能用于 $R = 0.1$ 情况下的疲劳寿命预测。

试验 S-N 曲线的疲劳强度大于 80 MPa, 该值仅表达试验中所用 Q235B 十字焊接接头的疲劳强度, 须进行修正, 弥补不同尺寸焊接试样间的残余应力偏差。可对试验疲劳强度采用式 (2) 进行修正, 应力循环比 $R = 0.1$, 疲劳增强系数为 0.86。

经验 S-N 曲线的疲劳强度属光滑试件的循环特性, 没有考虑焊接接头焊趾缺口处的应力集中, 可通过文献 [9] 提供的修正公式进行综合修正, 即

$$\sigma_h = \frac{\sigma_q}{K_f} \varepsilon \beta C_L \quad (6)$$

式中: σ_h 为修正后的应力; σ_q 为修正前的应力; K_f , ε , β , C_L 分别为疲劳缺口系数、尺寸系数、表面系数、载荷系数。根据有限元应力结果及文献 [9] 取 $K_f = 1.423$, $\varepsilon = 1$, 由于模拟过程没考虑试样表面情况, 所以取 $\beta = 0.9$, 与试验加载方式相同, 取 $C_L = 1$, 同时

该曲线是在 $R = -1$ 的情况下获取, 需要进行 Goodman 修正才可用于试验焊接接头的疲劳寿命预测。

3 横向十字接头疲劳寿命的数值模拟

利用软件 MSC. Fatigue 进行疲劳分析的流程如图 4 所示。

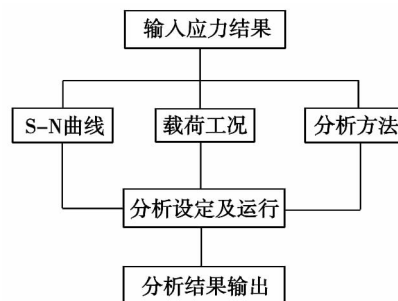


图 4 MSC. Fatigue 疲劳分析流程

Fig. 4 Process of fatigue analysis using MSC. Fatigue

根据图 2 可知, 接头的焊趾处应力集中较大, 所以疲劳危险部位处于焊趾。按照图 4 的分析流程, 把应力分析结果导入 MSC. Fatigue 前处理模块; 然后分别调用修正后的试验 S-N 曲线、标准 S-N 曲线和经验 S-N 曲线, 施加图 5 所示的循环载荷, 最后软件按照 Miner 线性疲劳损伤累积理论^[11] 运行全寿命疲劳分析。

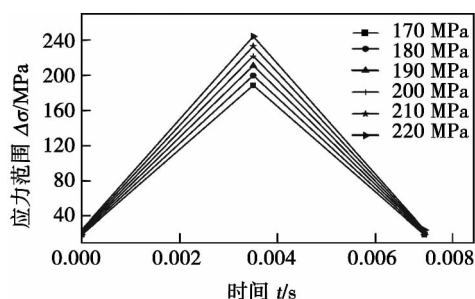


图 5 循环载荷

Fig. 5 Cyclic loading

MSC. Fatigue 可提供多种结果查询方式, 既有云图形式, 也可进行数据查询。表 5 为不同 S-N 曲线疲劳寿命的有限元数据结果。

依据表 5 数据作图 6 所示的寿命折线。由图 6 可见, 随着应力范围的增大, 3 条 S-N 曲线寿命预测值偏差越来越小。标准 S-N 曲线的预测值最小, 与试验 S-N 曲线预测值最大偏差为 28%, 最小偏差仅为 7.9%, 与经验 S-N 曲线的预测值最大为

表 5 疲劳寿命的有限元分析结果
Table 5 FEA results of fatigue life

| 名义应力范围 $\Delta\sigma_n/\text{MPa}$ | 疲劳寿命 $N(10^6 \text{ 周次})$ | | |
|---------------------------------------|---------------------------|-----------|-----------|
| | 标准 S-N 曲线 | 经验 S-N 曲线 | 试验 S-N 曲线 |
| 170 | 2.08 | 2.29 | 2.92 |
| 180 | 1.36 | 1.76 | 1.80 |
| 190 | 0.90 | 1.18 | 1.14 |
| 200 | 0.68 | 0.65 | 0.73 |
| 210 | 0.44 | 0.50 | 0.48 |

24% 最小为 3.8%; 而试验 S-N 曲线和经验 S-N 曲线的预测值相差不大, 在 3.3% ~ 19% 范围内。

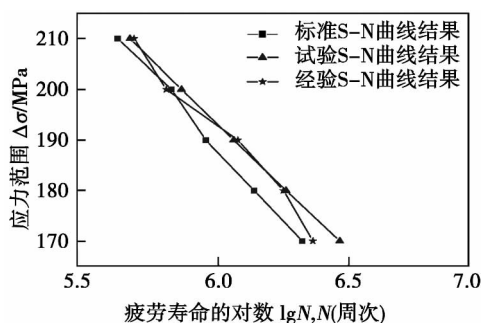


图 6 不同 S-N 曲线的疲劳寿命预测值

Fig. 6 Predictive value of fatigue life under different S-N curves

经分析可知 3 条 S-N 曲线预测的寿命值偏差不大, 试验 S-N 曲线一般只能用于相应焊接接头的疲劳寿命预测, 一旦接头形式稍有改变, 模拟结果将会出现很大的偏差。由于经验 S-N 曲线的预测值与试验 S-N 曲线的预测值相差不大, 所以可以断定经验 S-N 曲线的预测值具有一定的风险。而标准 S-N 曲线预测的寿命值相对偏小, 预测结果一般比较保守。

4 结 论

(1) 3 条 S-N 曲线在 2×10^6 周次循环时的疲劳强度相差很大, 说明未加修正的 S-N 曲线不能直接用于 Q235B 十字焊接接头的疲劳寿命预测。

(2) 试验 S-N 曲线预测值与经验 S-N 曲线预测值偏差较小, 经验 S-N 曲线预测值具有一定的危险性, 标准 S-N 曲线预测值相对保守。

(3) Q235B 十字焊接接头有限元寿命预测采用标准 S-N 曲线, 其结果更加安全。

参考文献:

- [1] 贾法勇, 霍立兴, 吴冰, 等. 双相不锈钢焊接接头疲劳强度[J]. 焊接学报, 2004, 25(2): 31-34.
Jia Fayong, Huo Lixing, Wu Bing, et al. Fatigue strength of duplex stainless steel welded joint[J]. Transactions of the China Welding Institution, 2004, 25(2): 31-34.
- [2] 武奇, 邱惠清, 王伟生. 基于结构应力的焊接接头疲劳分析[J]. 焊接学报, 2009, 30(3): 101-105.
Wu Qi, Qiu Huiqing, Wang Weisheng. Fatigue analysis of welded joints by method of structural stress[J]. Transactions of the China Welding Institution, 2009, 30(3): 101-105.
- [3] 于海丰, 张耀春, 杜守军. Q235 焊接工字形钢支撑的低周疲劳性能试验及数值模拟[J]. 四川大学学报, 2012, 44(2): 182-190.
Yu Haifeng, Zhang Yaochun, Du Shoujun. Experiment and numerical simulation on low-cycle fatigue behavior for Q235 welded I-section steel bracing members[J]. Journal of Sichuan University, 2012, 44(2): 182-190.
- [4] 王文先, 贺秀丽, 张红霞, 等. 基于 CDM 法 AZ31B 镁合金焊接接头疲劳评定[J]. 焊接学报, 2010, 31(10): 13-21.
Wang Wenxian, He Xiuli, Zhang Hongxia, et al. Fatigue assessment of welded joints of AZ31B magnesium alloy by using critical distance method[J]. Transactions of the China Welding Institution, 2010, 31(10): 13-21.
- [5] Hobbacher A. Recommendations for fatigue design of welded joints and components[S]. German: International Institute of Welding, 2002.
- [6] 周张义, 李 芾. 焊接残余应力对钢结构疲劳性能影响研究[J]. 机车电传动, 2009, 2(3): 24-29.
Zhou Zhangyi, Li Fu. Study on the effect of welding residual stresses on the fatigue behavior of steel structures[J]. Electric Drive for Locomotives, 2009, 2(3): 24-29.
- [7] Niemi E. Fatigue analysis of welded components[M]. UK: Woodhead Publishing Ltd, 2006.
- [8] 周传月, 郑红霞, 罗慧强, 等. MSC. Fatigue 疲劳分析应用与实例[M]. 北京: 科学出版社, 2005.
- [9] 王东锋, 汪定江, 王新坤. 构件安全疲劳寿命估算中的 P-S-N 曲线修正[C]// 中国航空学会. 第二届中国航空学会青年科技论坛文集(2). 洛阳, 2006: 507-513.

作者简介: 范文学, 男, 1981 年出生, 博士研究生, 讲师. 主要从事焊接疲劳和数控加工方面的科研和教学工作. 发表论文 5 篇.
Email: fw201878@163.com

通讯作者: 陈芙蓉, 女, 教授. Email: cfr7075@163.com

point of Al-Si moves to the Si side. It can be found that the phases in Al-Si-Zn brazed 6061 aluminum joint are α -Al, η -Zn, and Si particles, and the phases in Al-Si-Zn-Cu-P brazed seam are α -Al, η -Zn, fine Si particles, AlP phase.

Key words: modification; brazing; 6061 aluminum alloy; Si

Design of high power underwater laser cutting nozzle

XU Liang¹, WANG Wei¹, LI Xiaoyu¹, XU Yujun¹, LIU Shao-wei² (1. Harbin Welding Institute, China Academy of Machinery Science and Technology, Harbin 150028, China; 2. Shenyang Xinle Aerospace Co. Ltd., Shenyang 110034, China). pp 57–60

Abstract: According to the principle of the laser spot size requirement and the design principle of Laval nozzle, the part of stable section, contraction section, throat section and expansion section of the nozzle were designed. The size of stable section is mainly limited by the overall size of the laser cutting gun. Contraction section is used to connect the stable period and the throat section by using tangent arc transition. In order to ensure the laser go smoothly through the throat, throat diameter must be greater than the laser spot diameter. Expansion section adopts linear expansion method, in view of the cutting seam width limit, divergence angle should not be too large. According to the design size, the supersonic Laval nozzle was manufactured, the jet velocity and stiffness of oxygen flow was improved. In underwater laser cutting experiment, using the local drainage method and larger oxygen flow, 30 mm thick carbon steel plate was cut smoothly. Compared with the convergent nozzle, the cutting effect of the supersonic nozzle has been obviously improved

Key words: underwater; cutting; laser; nozzle

Effect of rare earth Ce on microstructure and properties of Zn-22Al filler metal

WANG Bo¹, LIU Han¹, XUE Song-bai¹, LI Yang¹, LOU Jiyuan², LOU Yinbin² (1. College of Materials Science and Technology, Nanjing University of Aeronautics and Astronautics, Nanjing 210016, China; 2. Zhejiang Xinrui Welding Material Co., Ltd., Shengzhou 312452, China). pp 61–64

Abstract: The effects of the rare earth Ce on the resistivity, melting temperature, spreadability, microstructure of Zn-22Al filler metal and shear strength of brazed joints were studied. The results indicated that the addition of Ce has little effect on the resistivity and the melting temperature of the filler metal. But with the addition of Ce, the spreadability is significantly improved, the microstructure is refined obviously. It has been found that Ce can improve the shear strength of Cu/Al joint notably. When the content of Ce is 0.05%, the spread area of filler metal on Al and Cu substrates reached maximum values, respectively, which are 21.4% and 11.6% higher than those of Zn-22Al alloy respectively. Moreover, the shear strength of Cu/Al joint brazed with Zn-22Al-0.05Ce reaches the peak value of 91.3 MPa, which is improved by 30.3% compared with the joint brazed with Zn-22Al alloy. However, with the addition of excessive amount of Ce, some brittle Ce-bearing phases appear in the microstructure and their sizes increase, and the spreadability of filler metal and shear strength of Cu/Al joint deteriorate significantly.

cantly.

Key words: rare earth Ce; Zn-Al filler metal; spreadability; microstructure; mechanical properties

Microstructure and mechanical properties of MIG welded joint of laser melting deposited TA15 titanium alloy

DU Borui, TIAN Xiangjun, WANG Huaming (School of Material Science and Engineering, Beihang University, Beijing 100191, China). pp 65–68

Abstract: Laser melting deposited (LMD) TA15 and rolled TA15 were welded by argon arc welding. The microstructure and phase constitution of the welded joint were studied by optical microscopy and scanning electron microscopy. The microhardness and mechanical properties of the welded joint were tested. The results indicate that the weld zone (WZ) mainly consists of columnar crystals with thick lamellar structure which epitaxially grow from the substrates. The grains in heat affected zone (HAZ) of rolled TA15 grow seriously because of its sensitivity to heat. The columnar grains in HAZ near weld zone of LMD TA15 turn into equiaxial grains. The microhardness of HAZ of LMD TA15 is the highest, while the WZ and HAZ of rolled TA15 is the lowest. The tensile strength of the welded joint is lower than that of both base metals, but the plasticity corresponds to the rolled TA15. Fracture position locates in the HAZ of rolled TA15.

Key words: titanium alloy; laser melting deposition; argon-arc welding; microstructure; mechanical properties

Fatigue life prediction of transverse cross welded joint based on different S – N curve

FAN Wenxue^{1,2}, CHEN Furong¹, XIE Ruijun¹, GAO Jian¹ (1. School of Materials Science and Engineering, Inner Mongolia University of Technology, Hohhot 010051, China; 2. School of Mining Institute, Inner Mongolia University of Technology, Hohhot 010051, China). pp 69–72

Abstract: Three kinds of S – N curves including experimental S – N curve, experience S – N curve and standard S – N curve were established by MSC. Fatigue software. The effects of residual stress, average stress and joint shape were considered. And these curves were revised according to the related criterion and used to predict the fatigue life of Q235B cross-shaped welded joint. The results show that, the fatigue damage locations of welded joint is consistent with that of experiment by S – N curve method based on MSC. Fatigue. The deviation is 7.9%–28% between the prediction values of experiment S – N curve and that of standard S – N curve. The deviation is 3.3%–19% between the prediction values of experiment S – N curve and that of experience S – N curve. The prediction values of experience S – N curve are higher than that of experiment S – N curve and that of standard S – N curve is more conservative.

Key words: cross welded joint; fatigue life; finite element analysis; S – N curve

Filler wire melting dynamics during laser beam welding with filler wire

LIU Hongbing¹, TAO Wang^{2,3}, CHEN Jie¹, YANG Zhibin², CHEN Lei¹, ZHAN Xiaohong¹, LI Liquan² (1.